

Effect of Inlet Velocity on Heat Transfer Process in a Novel Photo-Fermentation Biohydrogen Production Bioreactor using Computational Fluid Dynamics Simulation

Zhiping Zhang,^{a,b} Qinglin Wu,^b Chuan Zhang,^{a,c} Yi Wang,^a Yameng Li,^a and Quanguo Zhang^{a,*}

Temperature is one of the most important parameters in biohydrogen production by way of photo-fermentation. Enzymatic hydrolysate of corncob powder was utilized as a substrate. Computational fluid dynamics (CFD) modeling was conducted to simulate the temperature distribution in an up-flow baffle photo-bioreactor (UBPB). Commercial software, GAMBIT, was utilized to mesh the photobioreactor geometry, while the software FLUENT was adopted to simulate the heat transfer in the photo-fermentation process. The inlet velocity had a marked impact on heat transfer; the most optimum velocity value was $0.0036 \text{ m}\cdot\text{s}^{-1}$ because it had the smallest temperature fluctuation and the most uniform temperature distribution. When the velocity decreased from $0.0036 \text{ m}\cdot\text{s}^{-1}$ to $0.0009 \text{ m}\cdot\text{s}^{-1}$, more heat was accumulated. The results obtained from the established model were consistent to the actual situation by comparing the simulation values and experimental values. The hydrogen production simulation verified that the novel UBPB was suitable for biohydrogen production by photosynthetic bacteria because of its uniform temperature and lighting distribution, with the serpentine flow pattern also providing mixing without additional energy input, thus enhancing the mass transfer and biohydrogen yield.

Keywords: Enzymatic hydrolysate; Bioreactor; Computational fluid dynamics (CFD); Inlet velocity; Photo-fermentation biohydrogen production; Simulation; Temperature distribution

*Contact information: a: Key Laboratory of New Materials and Facilities for Rural Renewable Energy of Agricultural Ministry, Henan Agricultural University, Zhengzhou 450002, China; b: AgCenter, Louisiana State University, Baton Rouge 70803, USA; c: Institute of Electric Power, North China University of Water Resources and Electric Power, Zhengzhou 450011, China; *Corresponding author: zquanguo@163.com*

INTRODUCTION

Unrestrained utilization of fossil fuels has led to growing concerns over resource exhaustion, climate change, and environmental pollution. As a result, renewable energy sources need to be developed (US Energy Information Administration 2011). Hydrogen is a versatile, clean-burning, and high-specific energy (122 kJ g^{-1}) alternative energy source; its specific energy is almost three times greater than that of hydrocarbon fuels (Kapdan and Kargi 2006; Kapdan *et al.* 2009). Biological hydrogen production represents a sustainable resource because it utilizes various renewable sources such as waste water, biomass, and sunlight (Boran *et al.* 2010). Also, its production can take place at ambient process conditions that consume less energy (Asada and Miyake 1999). Biological hydrogen production can be separated into three approaches: biophotolysis of water, dark-fermentation, and photo-fermentation. Among these, photo-fermentation biohydrogen

production has the highest substrate conversion and can utilize the side products of dark-fermentation (*e.g.*, organic acids) (Hallenbeck 2011; Keskin *et al.* 2011; Adessi and De Philippis 2012). Nevertheless, the process suffers from a great number of restrictions. Much work is needed to develop a large-scale, economically attractive process (Hallenbeck *et al.* 2009).

Biohydrogen production is a complex, multiphase biological, chemical, and physical process with many internal interactions between gas, liquid, and solid phases. Present research on biohydrogen production has focused on the chemical and biological aspects that affect the efficiency of hydrogen production, while the physical characteristics such as reactor configuration and hydrodynamics have received very little attention (Ding *et al.* 2010). The key principles of photobioreactor design were well defined by Richmond (2004). Light supply, biomass concentration, mixing pattern, cell shear, temperature control, and mass transfer rate all influence the photobioreactor performance (Olivieri *et al.* 2014). Although various reactors have been developed, few studies have elucidated the heat transfer during the biohydrogen production process (Gavala *et al.* 2006; Cavalcante *et al.* 2009; Lee *et al.* 2009; Jung *et al.* 2011). Mixed photosynthetic bacteria are sensitive to temperature (Zhang and Shen 2006), so a stable environment is required for substrates utilization, light absorption, biomass growth, and bio-chemical reaction conduction. Photo-fermentation biohydrogen production is an enzymatic process, where accumulated heat is produced by the biochemical reaction and the incident light irradiation; this accumulated heat increases the temperature of the reactor, which possibly deactivates the microbial catalyst (Maskow *et al.* 2010). The dinitrogenase in the photosynthetic bacterium, which plays an important role in biohydrogen production, has activity in a narrow temperature range, generally between 30 and 37 °C. Thus, a dramatic temperature fluctuation can adversely influence biohydrogen production (Sasikala *et al.* 1993; Won and Lau 2011).

Knowing that heat is a key feature of life processes and has a marked impact on biohydrogen production, it is essential to monitor the heat transfer in the bioreactor in an effort to govern the microbial dynamics and reaction process. The hydrodynamics of the bioreactor has a great effect on the heat transfer and biohydrogen production. Modern computational fluid dynamics (CFD) is a method extensively employed for analyzing the bioreactor design, velocity fields, heat distributions, and mixing processes (Mortuza *et al.* 2011). Dhotre *et al.* (2005) conducted CFD simulation of steady state heat transfer in bubble columns. Sato *et al.* (2010) found that the microalgae productivity of bioreactors can be estimated before doing experiments using real algae. The CFD simulation technique can provide the flexibility to construct computational models that are easily adapted to diverse physical conditions without conducting experiment and predict the flow pattern and temperature distribution (Zhang and Li 2003; Dhotre and Joshi 2004).

CFD simulation technology has more utilization in the bioprocessing area, where insight into hydrodynamic and related phenomena, such as heat and mass transfer, can help manage risks and reduce the amount of expensive test rigs (Dhanasekharan 2006). The objective of this study was to optimize the heat transfer in the bioreactor to obtain higher cumulative hydrogen production. Enzymatic hydrolysate of corncob powder was utilized as the substrate for photo-fermentation hydrogen production. Computational fluid dynamics modeling was conducted to simulate the temperature distribution in an up-flow baffle photo-bioreactor (UBPB). To obtain uniform temperature distribution in the UBPB, commercial CFD software was employed to evaluate the influences of reactor configuration and inlet velocity on heat transfer. The temperature at different positions was monitored in the biohydrogen UBPB, and various inlet velocities were examined to

determine the optimum velocity for biohydrogen production. Computational fluid dynamics modeling was used to help reduce the number of experiments and govern the external factors such as illumination intensity, ambient temperature, flow pattern, reactor configuration.

EXPERIMENTAL

Materials and Methods

Microorganisms

The microorganisms used for photo-fermentation hydrogen production were originally isolated from a mixture of sewage sludge and fresh pig and cow dung (Han *et al.* 2013). Briefly, sewage sludge was obtained from a mesophilic anaerobic digester at the Wulongkou wastewater treatment works (Zhengzhou, Henan Province, China). Fresh pig and cow dung were obtained from the livestock farms belonging to the College of Veterinary Medicine at Henan Agricultural University. Sewage sludge (40 mL) and mixed pig and cow dung (200 mL) were incubated in a 1000-mL reagent bottle with a ground stopper. To this mixture was added the enrichment medium that contained the following components: NH_4Cl ($1 \text{ g}\cdot\text{L}^{-1}$), NaHCO_3 ($2 \text{ g}\cdot\text{L}^{-1}$), yeast extract ($1 \text{ g}\cdot\text{L}^{-1}$), K_2HPO_4 ($0.2 \text{ g}\cdot\text{L}^{-1}$), CH_3COONa ($3 \text{ g}\cdot\text{L}^{-1}$), $\text{MgSO}_4\cdot 7\text{H}_2\text{O}$ ($0.2 \text{ g}\cdot\text{L}^{-1}$), NaCl ($2 \text{ g}\cdot\text{L}^{-1}$), and 1 mL of a micronutrient solution ($\text{FeCl}_3\cdot 6\text{H}_2\text{O}$ ($5 \text{ mg}\cdot\text{L}^{-1}$), $\text{CuSO}_4\cdot 5\text{H}_2\text{O}$ ($0.05 \text{ mg}\cdot\text{L}^{-1}$), H_3BO_4 ($1 \text{ mg}\cdot\text{L}^{-1}$), $\text{MnCl}_2\cdot 4\text{H}_2\text{O}$ ($0.05 \text{ mg}\cdot\text{L}^{-1}$), $\text{ZnSO}_4\cdot 7\text{H}_2\text{O}$ ($1 \text{ mg}\cdot\text{L}^{-1}$), and $\text{Co}(\text{NO}_3)_2\cdot 6\text{H}_2\text{O}$ ($0.5 \text{ mg}\cdot\text{L}^{-1}$)). The pH value of the mixture was adjusted to 7.0. The growth of the photosynthetic bacteria (PSB) was conducted for four cycles that lasted for almost 30 d.

The phenotypic identification of the bacterial strains grown in this medium was carried out by 16S rDNA gene sequence analysis. The mixed strains sequences were analyzed by the Basic Local Alignment Search Tool (BLAST) comparative analysis method according to the National Center for Biotechnology Information (NCBI). The analysis showed that the mixed strains were *Rhodospirillum rubrum*, *Rhodobacter capsulatus*, and *Rhodopseudomonas palustris*.

Biomass pretreatment and enzyme

Corn cob powder pretreated with ball milling was provided by Key Laboratory of New Materials and Facilities for Rural Renewable Energy of Agricultural Ministry, China. The corn cob was harvested in the autumn of 2011 from a farm in Kaifeng city, Henan province. The natural corn cob was chopped to 0.5-1 cm size (moisture content of 8.9%), then it was crushed in a ball milling machine (Taichi Ring Nano Products Co., Ltd., Qinhuangdao, China) for 2 h. The mean particle size was $13.75 \mu\text{m}$, which was determined by LS 13 320 Laser Diffraction Particle Size Analyzer (Beckman Coulter, US). The corn cob powder after ball milling was kept airtight by ziplock bags and stored in a dark and dry place. The pretreated corn cob was utilized as the substrate in the entire work.

The cellulase that used in this studies was the Solarbio cellulase (enzyme activity of 30 U per mg, Japan).

Inoculum preparation

The growth medium for the mixed strains culture had the following composition: NH_4Cl ($1 \text{ g}\cdot\text{L}^{-1}$), NaHCO_3 ($2 \text{ g}\cdot\text{L}^{-1}$), yeast extract ($1 \text{ g}\cdot\text{L}^{-1}$), K_2HPO_4 ($0.2 \text{ g}\cdot\text{L}^{-1}$), CH_3COONa ($4 \text{ g}\cdot\text{L}^{-1}$), $\text{MgSO}_4\cdot 7\text{H}_2\text{O}$ ($0.2 \text{ g}\cdot\text{L}^{-1}$), and NaCl ($2 \text{ g}\cdot\text{L}^{-1}$).

The substrate solution utilized for photo-fermentation consisted of reducing sugars obtained from the enzymatic hydrolyzate of corncob powder, which was used as the carbon source. Carbon, nitrogen, phosphorous, and micro-nutrients of the fermentation medium were supplied in the following dosages: NH_4Cl ($0.4 \text{ g}\cdot\text{L}^{-1}$), K_2HPO_4 ($0.5 \text{ g}\cdot\text{L}^{-1}$), MgCl_2 ($0.2 \text{ g}\cdot\text{L}^{-1}$), yeast extract ($0.1 \text{ g}\cdot\text{L}^{-1}$), NaCl ($2 \text{ g}\cdot\text{L}^{-1}$), and sodium glutamate ($3.56 \text{ g}\cdot\text{L}^{-1}$). The inoculum load of bacteria during the logarithmic phase was 20% (v/v).

Reactor configuration and operating conditions

Photo-fermentation efficiency is highly dependent on the operating conditions and photobioreactor design. In this study, a novel continuous up-flow plate reactor with horizontal baffles was employed. The up-flow baffle bioreactor (UBPB) can provide mixing without additional energy input (Chen *et al.* 2011). It is made from polymethyl methacrylate, which light can penetrate. Light emitting diode (LED) was utilized to illuminate the photobioreactor system because of its advantages over conventional lighting, such as higher energy efficiency, narrow wavelength emission spectra appropriate for biomass growth, ease of operation, long life-expectancy, and low irradiation heating (Nedbal *et al.* 2008; Tamburic *et al.* 2011). To shorten the light path and to enhance the light penetration, the lamps plates were located in the hollow baffles with a light intensity of 3000 lx, which corresponded to $0.88 \text{ W}\cdot\text{L}^{-1}$.

The schematic of the photo-fermentation hydrogen production system and up-flow baffle bioreactor are shown in Fig. 1. Figure 1a illustrates the system components, which are made up of six units. The feed unit consists of a photosynthetic bacteria container, a fermentative substrate container, and two peristaltic pumps. The premixed unit mixes the PSB and fermentative substrate before the solutions are pumped into the fermenter. The gas collection unit has a gas bag, a liquid effluent container, and gas-liquid separation. The fermentation solution utilized for biohydrogen production was premixed and pumped into the photo-bioreactor. Then, the reactors were sealed and purged with nitrogen gas (N_2) for 2 min to create an anaerobic environment. After reaction, the remaining solution flowed from the discharge hole for reutilization or disposal, and the biogas produced in the bioreactor was collected in air bags using the air outlet.

Figure 1b depicts the structure of the UBPB. Two baffles equally divide the fermenter tank into three units. The baffles were attached alternately to the front and the back of the larger flat faces of the reactor. The wall of both ends and the baffles are hollow and transparent, which allow the two-sided LED lamps plates to be located within.

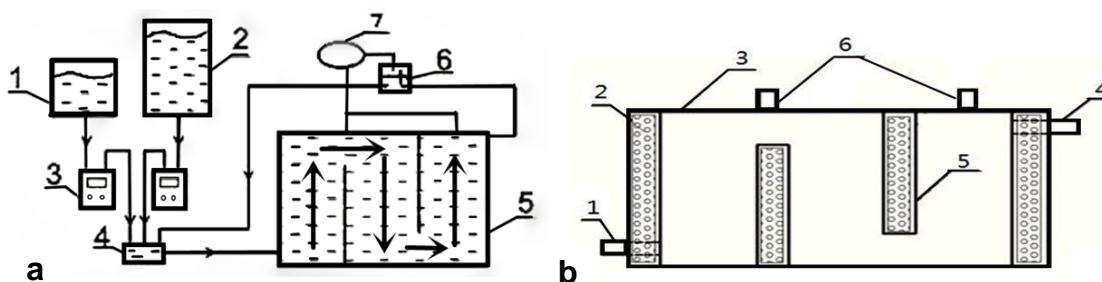


Fig. 1. Schematic of the photo-fermentation hydrogen production system and the up-flow baffle bioreactor. (a) 1-Photosynthetic bacteria container; 2-fermentative substrate container; 3-peristaltic pump; 4- premixed unit; 5-UBPB unit; 6-liquid effluent container; and 7-gas-liquid separation gas bag. (b) 1-Substrate feed inlet; 2-LED lamps plate; 3-fermentative unit; 4-discharge hole; 5-baffle plate; and 6-air outlet

The overall dimensions of the UBPB are 0.26 m in length, 0.1 m in width, and 0.16 m in height; the dimensions of the baffles are 0.02 m in length, 0.1 m in width, and 0.14 m in height. The pipe diameters are 0.01 m. The height of the discharge hole is 0.15 m, and the effective volume is 0.0027 m³.

Operation of the continuous up-flow baffle bioreactor

The operation parameters were set according to the values that have been determined previously (Zhang *et al.* 2014). Enzymatic hydrolyzate produced from the corncob powder was utilized as fermentative substrate with a fixed initial concentration of 10.5 g reducing sugar•L⁻¹ solution. The reducing sugar contained in substrate was the carbon source utilized by the PSB for growth and metabolism. The fermentation medium was added to the fermentation solution in the following dosages: NH₄Cl (0.4 g•L⁻¹), K₂HPO₄ (0.5 g•L⁻¹), MgCl₂ (0.2 g•L⁻¹), yeast extract (0.1 g•L⁻¹), NaCl (2 g•L⁻¹), and sodium glutamate (3.56 g•L⁻¹). The initial pH value of the mixture was adjusted to 7 by the addition of 50% KOH solution (m/m). The pre-cultured PSB, which were in the logarithmic phase, were added to the photo-fermentation substrate solution for hydrogen production. The volume ratio of PSB to fermentation substrate was 1:4.

The prepared fermentation solutions were pumped into the bioreactors. The inlet velocity was set at different level in order to obtain diverse flow conditions. All continuous UBPBs with continuous illumination (3000 lx, or 0.88 W•L⁻¹) and controlled temperature at 30 ± 1 °C were carried out in a digital biochemical incubator (SPX-250B-III, Midwest Group; Shanghai, China). The time period of biohydrogen production was four days. Every experiment was replicated twice.

Analytical methods

The efficiency of photo-fermentation for biohydrogen production was evaluated with respect to the temperature distribution and the biohydrogen yield. The temperature was measured using an online data logger thermometer (YC-747UD, Yu Ching Technology Co., Ltd.; Taipei City, Taiwan), accuracy of ±0.1 °C, connected to a computer for collecting the data. The temperature sensors were placed at the feed inlets, discharge holes, center of reactor, and reactor walls.

Hydrogen gas was collected in airbags. The volume and composition of cumulative hydrogen production were determined by gas chromatography (6820 GC-14B, Agilent Technologies; Beijing, China). The specific heat and thermal conductivity of the fermentation solutions (at 30 °C) were determined with a comprehensive thermal analyzer (STA 449 C Jupiter DSC-TG, Netzsch-Gerätebau GmbH; Germany). Dynamic viscosity was measured using a rotary digital viscometer (NDJ-5S, Rinch Industrial Co., Ltd.; Shanghai China). Density was determined by a digital densitometer (HJ33-DMA4000, Anton Paar (Shanghai) Trading Co., Ltd.; Shanghai, China).

The substrate conversion efficiency was calculated according to Eq. 1,

$$\text{Substrate conversion efficiency} = [(Y_{\text{initial}} - Y_{\text{final}})/Y_{\text{initial}}] \times 10 \quad (1)$$

where Y_{initial} is the initial reducing sugar yield and Y_{final} is the reducing sugar yield at the end of the reaction. The reducing sugar concentration was determined by the DNS method of Miller (1959) using a spectrophotometer (HP8453 Ultraviolet Spectrophotometer, Agilent Technologies; USA) at a wavelength of 540 nm. The reducing sugar yield (Y) was

calculated from the absorbance (x) using a glucose standardization curve based on the following regression equation (with $r^2 = 0.9990$):

$$Y = 0.3580 \cdot x - 0.0164 \quad (2)$$

Simulation and assumptions

Computational fluid dynamics simulation includes geometry creation, mesh generation, boundary condition set up, and finally iterative solution of the governing radiative transfer equation (RTE) (Sahu *et al.* 2011). GAMBIT 2.4.6 software (ANSYS Inc.; Cecil Township, PA) was employed to mesh the photobioreactor geometry, and the uncoupled implicit 2D solver software FLUENT 6.3.26 (Fluent Inc.; Lebanon, NH, USA) was used to solve the equations governing the system for simulating the temperature distribution. The flow was an incompressible stationary flow. The simulations were carried out on a PC equipped with an Intel Xeon 2.4 GHz processor and 8 GB of RAM.

The following assumptions were made for the two-dimensional simulation of the heat distribution in the UBPB at steady-state conditions: (1) The temperature gradient happens in the lengthwise direction because the light has the same distribution in the crosswise direction (so the model is simplified to 2D); (2) The free surface in the fermenter was set to solid wall, because the normal velocity of the free surface can be ignored; (3) The heat exchange just focused on the convection heat transfer between the walls and the inflow substrate; (4) The pressure in the UBPB was constant at atmospheric pressure because the produced biogases were all discharged through the gas outlet and collected by a constant pressure air bag. The viscosity, thermal conductivity, density, and specific heat of the fermentation solutions were assumed to be constant because the temperature differentials are small; and (5) The fluid flow inside the UBPB was fully developed and no disturbance and back mixing occurred.

Boundary conditions and convergent condition

The inlet fluid velocity and temperature at the inlet are known. Different inlet velocities were assigned by the peristaltic pump as $0.0036 \text{ m}\cdot\text{s}^{-1}$, $0.0027 \text{ m}\cdot\text{s}^{-1}$, $0.0018 \text{ m}\cdot\text{s}^{-1}$, and $0.0009 \text{ m}\cdot\text{s}^{-1}$, which were calculated by dividing the volume flow rate by the inlet cross sectional area. The outlet of the fermentation solutions was set as a static pressure (*i.e.*, atmospheric pressure). The remaining boundaries of the model were left as default wall boundary conditions, and no slip occurred at the wall. Model parameters applied for the CFD simulation were as follows: solution density (ρ) was $1125 \text{ kg}\cdot\text{m}^{-3}$; viscosity (ν) was $1.3 \times 10^{-3} \text{ kg}\cdot\text{m}^{-1}\cdot\text{s}^{-1}$; specific heat (c_p) was $5.167 \text{ kJ}\cdot\text{kg}^{-1}\cdot\text{K}^{-1}$; and thermal conductivity (λ) was $0.63 \text{ W}\cdot\text{m}^{-1}\cdot\text{K}^{-1}$. The relative error was specified using a convergence criterion of 10^{-5} for each scaled residual component.

RESULTS AND DISCUSSION

Geometrical Details

The grid generation or meshing of the UBPB fermenter is depicted in Fig. 2, which is also the two-dimensional computational domain utilized in the simulations. The computational grid consisted of 1058 nodes, 928 quadrilateral cells, and 1985 faces (252 mixed wall faces, 3 mixed pressure-outlet faces, 3 mixed velocity-inlet faces, and 1727 mixed interior faces).

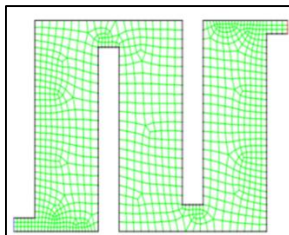


Fig. 2. Meshing of the UBPB fermenter

Model Validation

The solver model was chosen as a pressure-based solver, with implicit and absolute velocity formulation. Since the UBPB has an axial symmetry shape, the space type is 2D, steady flow. The gradient option in FLUENT was Green-Gause Cell Based.

The Reynolds number (Re) was utilized to determine the flow regime and is calculated as,

$$Re = \frac{\rho v D}{\eta} \quad (3)$$

where ρ is density, v is velocity, D is inlet diameter, and η is viscosity. Because $Re \ll 2000$, the viscous model determined that the flow was laminar, where the fluid side heat transfer is approximated as,

$$q'' = k \frac{\partial T}{\partial n} \approx k \left. \frac{\Delta T}{\Delta n} \right|_n \quad (4)$$

where n = local coordinate normal to the wall.

The energy equation was also utilized to activate calculation of heat transfer. In order to include viscous heating terms in the energy equation, Viscous Heating in Viscous Model panel in FLUENT was switched on. The material properties for heat transfer and thermal boundary conditions were defined. The operating pressure was 101.325 kPa, gravitational acceleration was $-9.8 \text{ m}\cdot\text{s}^{-2}$; the temperature of the inlet (velocity-inlet) and outlet (pressure-outlet) were determined by a thermometer.

After the pre-processing, the model was utilized to simulate the temperature distribution of the biohydrogen production system at different inlet velocities to investigate the effects of the inlet velocity on heat transfer and hydrogen production.

Temperature Field Evaluation

The model solve in FLUENT was based on the discretization of solution controls, and need to select the options as follows: standard pressure, first order upwind momentum and energy, residual monitors. After iterative computations, temperature fields were reported by the surface monitors, and temperature distribution at different inlet velocities were obtained as shown in Fig. 3. The temperature scale on the left of each image can be used to determine the temperature of the fermentative solution.

Steady-state simulations at four levels of inlet velocity were conducted to optimize the operation of the photobioreactor. Figure 3 presents the temperature distribution in the reaction zone of the UBPB with various inlet velocities. The simulation results demonstrate that temperature distribution differs due to the diverse inlet velocities. Higher temperature means more heat was accumulated. When the inlet velocity was $0.0036 \text{ m}\cdot\text{s}^{-1}$, the

temperature fluctuation was small, which indicates a uniform temperature throughout the biohydrogen production process. The temperature variation increased as the inlet velocity decreased.

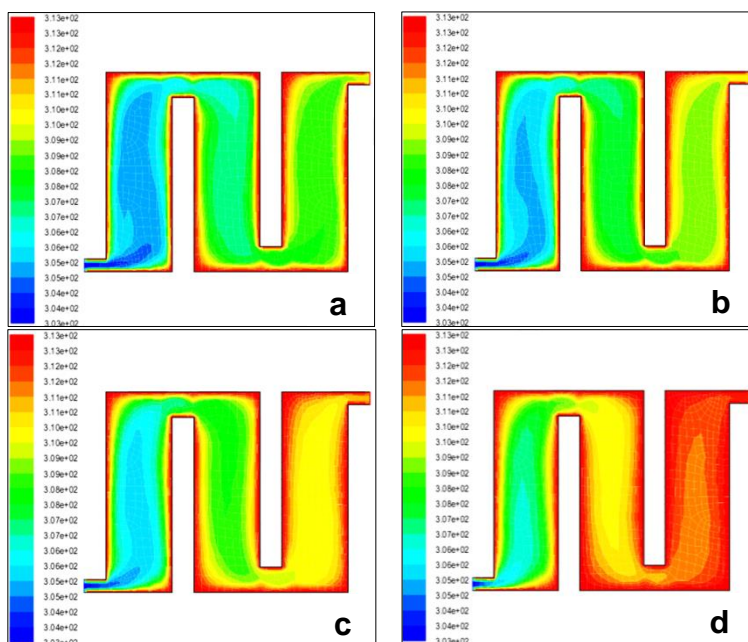


Fig. 3. The temperature distribution in the reactor at different inlet velocities: (a) $0.0036 \text{ m}\cdot\text{s}^{-1}$; (b) $0.0027 \text{ m}\cdot\text{s}^{-1}$; (c) $0.0018 \text{ m}\cdot\text{s}^{-1}$; and (d) $0.0009 \text{ m}\cdot\text{s}^{-1}$

Figure 3 also demonstrates that the temperature of the fermentation solutions increased along the reactor's flow path. Natural heat convection occurred between the high-temperature walls and the low-temperature fermentation solutions. Photo-fermentation requires light throughout the entire process of biochemical reaction; only a minor fraction of the light energy is absorbed and utilized by the photosynthetic bacteria, while most is dissipated as heat (Mukhanov and Kemp 2006). The walls remain at a high temperature because of the direct absorption of radiation.

Temperature fluctuations are an important factor affecting hydrogen production (Boran *et al.* 2010). The $0.0036 \text{ m}\cdot\text{s}^{-1}$ is the most optimal inlet velocity among the selected values because the reactor has a uniform temperature distribution. As the inlet velocity was decreased from $0.0036 \text{ m}\cdot\text{s}^{-1}$ to $0.0009 \text{ m}\cdot\text{s}^{-1}$, the outlet temperatures increased to 35.9, 37.1, 38.7, and 40.2 °C. These temperatures are in the suitable temperature range of biohydrogen production, except for the $0.0009 \text{ m}\cdot\text{s}^{-1}$ inlet velocity. In each part divided by the baffles, the temperature difference between the center and edge regions were minimal, which indicated that the LED lighting system can provide balanced illumination throughout the bioreactor. The LED lamps not only provide light, but also maintain the reaction in the appropriate temperature range. Thus, this novel bioreactor is suitable for biohydrogen production using photosynthetic bacteria, and this optimized lighting system significantly reduces the cost of the bioprocess.

Comparison of Simulated and Experimental Results

Comparisons between simulated values and experimental values at different inlet velocity were conducted. The results are shown in Fig. 4.

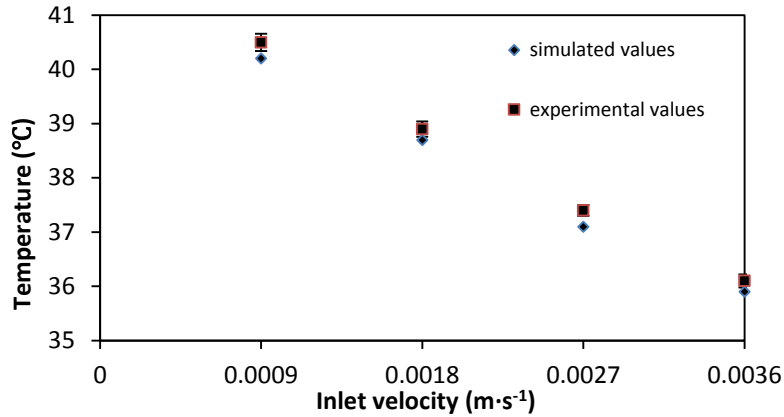


Fig. 4. Comparisons between simulated and experimental values at different inlet velocities

Qualitatively, the numerical solutions of the CFD model agreed well with the experimental results, which indicated that the established model is consistent with the actual system and is capable of accurately predicting the temperature distribution within the photo-fermentation reactor.

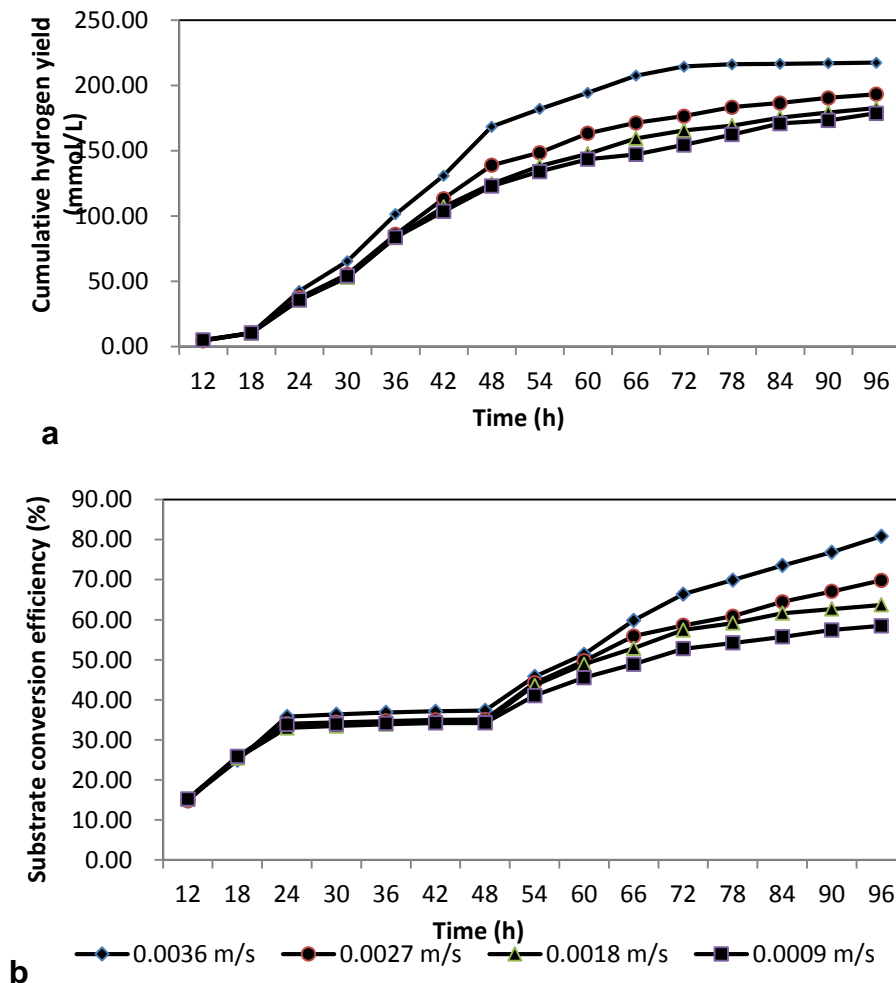


Fig. 5. (a) Cumulative hydrogen yield and (b) substrate conversion efficiency at different inlet velocities in the UBPB reactor

The CFD simulation method can help optimize the biochemical process in bioreactors by quantifying flow fields and heat transfer characteristics, monitoring the changes and risks during the scale-up, and reduce costs with proper design (Dhanasekharan 2006).

Hydrogen Production Analysis

The cumulative hydrogen yield (Fig. 5a) and substrate conversion (Fig. 5b) in the UBPB reactor increased with an increase in inlet velocities. From the experimental data, it can be seen that when the inlet velocity was $0.0036 \text{ m}\cdot\text{s}^{-1}$, the hydrodynamic and thermodynamic behaviors of the bioreactor were suitable for biohydrogen production. The highest cumulative hydrogen yield and substrate conversion efficiency were obtained at this velocity. This observation suggests that a fast inlet velocity provides better heat transfer in the UBPB reactor and this behavior yields a uniform temperature distribution, which is beneficial for growth and metabolism of the PSB.

CONCLUSIONS

1. Enzymatic hydrolysate of corncob powder was utilized as a substrate for biohydrogen production. A novel up-flow baffle photobioreactor was adapted and shown to be suitable for hydrogen production.
2. Temperature distributions in the photobioreactor were analyzed to obtain high hydrogen yield. A 2D CFD model for photo-fermentation hydrogen production was used to optimize the heat transfer in the UBPB bioreactor.
3. Different inlet velocities were examined to determine their effect on the temperature distribution in the UBPB reactor. A slow inlet velocity intensified heat accumulation, which was adverse to the growth and metabolism of the photosynthetic bacteria and had the lowest cumulative hydrogen yield. The inlet velocity of $0.0036 \text{ m}\cdot\text{s}^{-1}$ was the most optimum among the selected inlet velocity because it had the most uniform temperature distribution throughout the bioreactor.
4. By integrating the results of simulations with experimental observations, it is clearly shown that the results obtained from the established model are consistent to the actual situation, in which the UBPB reactor is a good model for biohydrogen production by photosynthetic bacteria.

ACKNOWLEDGMENTS

This work was supported by the National Natural Science Foundation of China (51376056) and the National High Technology Research and Development Program (*i.e.*, 863 Program) of China (2012AA051502).

REFERENCES CITED

- Adessi, A., and De Philippis, R. (2012). "Hydrogen production: Photofermentation," in: *Microbial Technologies in Advanced Biofuels Production*, P. C. Hallenbeck (ed.), Springer, New York, pp. 53-75.
- Asada, Y., and Miyake, J. (1999). "Photobiological hydrogen production," *J. Biosci. Bioeng.* 88(1), 1-6. DOI: 10.1016/S1389-1723(99)80166-2
- Boran, E., Özgür, E., van der Burg, J., Yücel, M., Gündüz, U., and Eroglu, I. (2010). "Biological hydrogen production by *Rhodobacter capsulatus* in solar tubular photo bioreactor," *J. Clean. Prod.* 18(S1), S29-S35. DOI: 10.1016/j.jclepro.2010.03.018
- Chen, C. Y., Liu, C. H., Lo, Y. C., and Chang, J. S. (2011). "Perspectives on cultivation strategies and photobioreactor designs for photo-fermentative hydrogen production," *Bioresour. Technol.* 102(18), 8484-8492. DOI: 10.1016/j.biortech.2011.05.082
- Dhanasekharan, K. (2006). "Design and scale-up of bioreactors using computer simulations," *Bioproc. Int.* 4(3), 34-41.
- Dhotre, M. T., and Joshi, J. B. (2004). "Two-dimensional CFD model for the prediction of flow pattern, pressure drop and heat transfer coefficient in bubble column reactors," *Chemical Engineering Research and Design* 82(6), 689-707. DOI: 10.1205/026387604774195984
- Dhotre, M. T., Vitankar, V. S., and Joshi, J. B. (2005). "CFD simulation of steady state heat transfer in bubble columns," *Chemical Engineering Journal* 108(1-2), 117-125. DOI: 10.1016/j.cej.2005.01.006
- Ding, J., Wang, X., Zhou, X. F., Ren, N. Q., and Guo, W. Q. (2010). "CFD optimization of continuous stirred-tank reactor for biohydrogen production," *Bioresour. Technol.* 101(18), 7005-7013. DOI: 10.1016/j.biortech.2010.03.146
- Gavala, H. N., Skiadas, L. V., and Ahring, B. K. (2006). "Biological hydrogen production in suspended and attached growth anaerobic reactor systems," *Int. J. Hydrogen Energ.* 31(9), 1164-1175. DOI: 10.1016/j.ijhydene.2005.09.009
- Hallenbeck, P. C. (2011). "Microbial paths to renewable hydrogen production," *Biofuels* 2(3), 285-302. DOI:10.4155/bfs.11.6
- Hallenbeck, P. C., Ghosh, D., Skonieczny, M. T., and Yargeau, V. (2009). "Microbiological and engineering aspects of biohydrogen production," *Indian J. Microbiol.* 49(1), 48-59. DOI: 10.1007/s12088-009-0010-4
- Han, B. X., Wang, Y., Zeng, F., and Zhang, Q. G. (2013). "Enrichment predominant group of hydrogen-producing photosynthetic bacteria and their hydrogen production experiment," *Acta Energ. Solar. Sin.* 34(1), 111-115.
- Jung, K. W., Kim, D. H., Kim, S. H., and Shin, H. S. (2011). "Bioreactor design for continuous dark fermentative hydrogen production," *Bioresour. Technol.* 102(18), 8612-8620. DOI: 10.1016/j.biortech.2011.03.056
- Kapdan, I. K., and Kargi, F. (2006). "Bio-hydrogen production from waste materials," *Enzyme Microb. Technol.* 38(5), 569-582. DOI: 10.1016/j.enzmictec.2005.09.015
- Kapdan, I. K., Kargi, F., Oztekin, R., and Argun, H. (2009). "Bio-hydrogen production from acid hydrolyzed wheat starch by photo-fermentation using different *Rhodobacter sp.*," *Int. J. Hydrog. Energ.* 34(5), 2201-2207. DOI: 10.1016/j.ijhydene.2009.01.017
- Keskin, T., Abo-Hashesh, M., and Hallenbeck, P. C. (2011). "Photofermentative hydrogen production from wastes," *Bioresour. Technol.* 102(5), 8557-8568. DOI: 10.1016/j.ijhydene.2009.01.017

- Lee, D. Y., Li, Y. Y., and Noike, T. (2009). "Continuous H₂ production by anaerobic mixed microflora in membrane bioreactor," *Bioresour. Technol.* 100(8), 690-695. DOI: 10.1016/j.ijhydene.2006.09.018
- Maskow, T., Kemp, R., Buchholz, F., Schubert, T., Kiesel, B., and Harms, H. (2010). "What heat is telling us about microbial conversions in nature and technology: From chip to megacalorimetry," *Microb. Biotechnol.* 3(3), 269-284. DOI: 10.1111/j.1751-7915.2009.00121.x
- Miller, G. (1959). "Use of dinitrosalicylic acid reagent of determination of reducing sugar," *Anal. Chem.* 31(3), 426-428. DOI: 10.1021/ac60147a030
- Mortuza, S. M., Kommareddy, A., Gent, S. P., and Anderson, G. A. (2011). "Computation and experimental investigation of bubble circulation patterns within a column photobioreactor," in: *ASME 5th International Conference on Energy Sustainability*, Washington, DC, August 7-10, 2011, Paper No. ES2011-54205, pp. 1131-1140. DOI: 10.1115/ES2011-54205
- Mukhanov, V. S., and Kemp, R. B. (2006). "Simultaneous photocalorimetric and oxygen polarographic measurements on *Dunaliella maritima* cells reveal a thermal discrepancy that could be due to nonphotochemical quenching," *Thermochim. Acta* 446(1-2), 11-19. DOI: 10.1016/j.tca.2006.03.018
- Nedbal, L., Trtilek, M., Cervený, J., Komarek, O., and Pakrasi, H. B. (2008). "A photobioreactor system for precision cultivation of photoautotrophic microorganisms and for high-content analysis of suspension dynamics," *Biotechnol. Bioeng.* 100(5), 902-910. DOI: 10.1002/bit.21833
- Olivieri, G., Salatino, P., and Marzocchella, A. (2014). "Advances in photobioreactors for intensive microalgal production: configurations, operating strategies and applications," *J. Chem. Technol. Biotechnol.* 89(2), 78-195. DOI: 10.1002/jctb.4218
- Richmond, A. (2004). "Biological principles of mass cultivation," in: *Handbook of Microalgal Culture: Biotechnology and Applied Phycology*, A. Richmond (ed.), Wiley-Blackwell, London, pp. 125-177.
- Sahu, A. K., Vasumathi, K. K., and Premalatha, M. (2011). "Simulation of solar light intensity distribution in open pond photobioreactor," *Int. J. Curr. Sci.* 1, 50-57.
- Sasikala, K., Ramana, C. V., Raghuvēer, R. P., and Kovacs, K. L. (1993). "Anoxygenic phototrophic bacteria: Physiology and advances in hydrogen production technology," in: *Advances in Applied Microbiology*, S. Neidleman and A. I. Laskin (eds.), Academic Press, New York, pp. 211-295. DOI: 10.1016/S0065-2164(08)70217-X
- Sato, T., Yamada, D., and Hirabayashi, S. (2010). "Development of virtual photobioreactor for microalgae culture considering turbulent flow and flashing light effect," *Energy Conversion and Management* 51(6), 1196-1201. DOI: 10.1016/j.enconman.2009.12.030
- Tamburic, B., Zemichael, F. W., Crudge, P., Maitland, G. C., and Hellgardt, K. (2011). "Design of a novel flat-plate photobioreactor system for green algal hydrogen production," *Int. J. Hydrog. Energ.* 36(11), 6578- 6591. DOI: 10.1016/j.ijhydene.2011.02.091
- US Energy Information Administration (2011). *International Energy Outlook 2011*, Report No.: DOE/EIA-0484, U.S. Dept. of Energy, Washington, DC, [www.eia.gov/ieo/pdf/0484\(2011\).pdf](http://www.eia.gov/ieo/pdf/0484(2011).pdf) , Accessed on September 19, 2011.
- Won, S. G., and Lau, A. K. (2011). "Effects of key operational parameters on biohydrogen production via anaerobic fermentation in a sequencing batch reactor," *Bioresour. Technol.* 102(13), 6876-6883. DOI: 10.1016/j.biortech.2011.03.078

- Zhang, Y., and Shen, J. (2006). "Effect of temperature and iron concentration on the growth and hydrogen production of mixed microflora," *Int. J. Hydrog. Energ.* 31(4), 441-446. DOI: 10.1016/j.ijhydene.2005.05.006
- Zhang, Z., and Li, Y. (2003). "CFD simulation on inlet configuration of plate-fin heat exchangers," *Cryogenics* 43(12), 673-678. DOI: 10.1016/S0011-2275(03)00179-6
- Zhang, Z. P., Yue, J. Z., Zhou, X. H., Jing, Y. Y., Jiang, D. P., and Zhang, Q. G. (2014). "Photo-fermentative bio-hydrogen production from agricultural residue enzymatic hydrolyzate and the enzyme reuse," *BioResources* 9(2), 2299-2310. DOI: 10.15376/biores.9.2.2299-2310

Article submitted: August 13, 2014; Peer review completed: October 5, 2014; Revised version received and accepted: November 4, 2014; Published: November 24, 2014.